Effects of Electrostatic Interactions on Orientational Order of Solutes in Liquid Crystals

Andrea di Matteo,† Alberta Ferrarini,* and Giorgio J. Moro‡

Dipartimento di Chimica Fisica, Università di Padova 2 via Loredan, 35131 Padova, Italy

Received: March 7, 2000; In Final Form: June 7, 2000

A mean-field model for the analysis of electrostatic interactions in liquid crystal phases is proposed. The model is based on a realistic description of the probe molecule and a continuum approximation for its environment. Electrostatic interactions, treated with the reaction field model, are superimposed to short-range interactions, which are accounted for by a shape method. The model is used to predict orientational order parameters of some representative solutes, characterized by different shapes and charge distributions, dissolved in nematics with different dielectric permittivities.

I. Introduction

Analysis of electrostatic interactions in liquid crystal phases is of interest for several reasons, the first of which is the assessment of their role in the mesophase ordering. The nature of the interactions responsible for the existence of liquid crystal phases has been a matter of debate for a long time, with theories tracing back the origin of mesophases to different interactions. As examples it is worth mentioning the successful theories developed by Onsager[1] and Maier-Saupe[2] based, respectively, on excluded volume and dispersion interactions and the early model developed by Born,[3] invoking dipolar forces between molecules as the driving mechanism for the formation of liquid crystalline phases. Nowadays, the dominant role of short-range interactions, which are modulated by the molecular shape, is generally recognized. On the other hand, electrostatic interactions, although not necessary to explain the existence of mesophases, might have relevant effects on properties like transition temperatures and phase sequence. The presence of dipoles is known to affect the structure of smectic phases and has particular relevance for the occurrence of reentrant[4] and ferroelectric[5] liquid crystal phases. Of course, electrostatic interactions determine the dielectric properties of mesophases and their response to electric fields, knowledge of which is important for application purposes.

The effects of electrostatic interactions on the structure and phase behavior of liquid crystals have been investigated theoretically by many authors by using various methods, e.g., computer simulations, density functional theories, and mean-field approaches (for a recent review see ref 6). Most studies, aimed at understanding their influence on the phase behavior, employ a simplified representation, with dipolar interactions for the electrostatic forces and simple axial objects for the molecular shape.[7] On the contrary, we intend to include a detailed and realistic description of the molecular properties within a mean-field approach. The mean-field potential experienced by a molecule in the liquid crystal phase is written as the superimposition of short-range and electrostatic interactions. The former are accounted for by the *surface tensor* approach, a shape model formulated some years ago[8] and successfully applied to predict molecular order parameters and transitional properties in nematics[9] as well as the helical pitch of chiral nematics.[10,11] Electrostatic interactions are described by the *reaction field* model for the coupling between the molecular charge distribution, within a cavity identified with the volume occupied by the molecule, and the electric field generated by the surrounding polarizable dielectric.[12] The reaction field approximation is widely used in the study of solvation effects, both in connection with a quantum mechanical treatment of the molecular systems[13] and with a simpler description in terms of point charges and localized polarizabilities, suitable for more complex biological molecules.[14,15] The method has also been applied to liquid crystals by taking into account the dielectric anisotropy.[16,17] In the present work the reaction field is expressed according to a method recently developed in the quantum mechanical study of solvation,[18,19] which leads to the reformulation of the problem as the interaction between the potential generated by the charge distribution of the molecule and apparent charges induced on the molecular surface. Our implementations of the reaction field model and of the surface tensor have the common feature that the molecular properties of the probe molecule, in particular its surface and charge distribution, are taken into account in detail. On the other hand, the medium is viewed as a continuum, affecting the probe only through its macroscopic properties, i.e., its orienting strength and dielectric permittivity.

By following such an approach, we shall analyze specifically the effects of electrostatic interactions on orientational ordering of solutes in nematics. Solutes in liquid crystal solvents have been shown to be very useful to probe the properties of the anisotropic environment. The convenience derives from the possibility of choosing simple molecules, the behavior of which is more easily understood than that of mesogenic systems, which usually are flexible and lack any symmetry. Another advantage is that the effects under investigation can be emphasized (or depressed) by appropriately changing the solute or the liquid crystal solvent. Information on orientational order of solutes, commonly described in terms of the Saupe ordering matrix $\boldsymbol{S}$,[20] can be obtained with optical and magnetic spectroscopy techniques using the solutes as probes. In particular, from NMR spectra the whole Saupe matrix can be determined provided that the molecule contains a sufficient number of independent sites.[21] It has been shown that *shape models*, derived in different ways but with the common feature that interactions are modeled on the basis of the molecular shape, are able to explain the

* Corresponding author. E-mail: a.ferrarini@chfi.unipd.it.
† E-mail: a.di.matteo@chfi.unipd.it.
‡ E-mail: g.moro@chfi.unipd.it.

10.1021/jp000891x CCC: $19.00
Published on Web 07/26/2000

orientational behavior of solutes in liquid crystals (cf. ref 22 and references therein). This is one of the arguments in favor of the aforementioned conclusion that short-range interactions are the dominant mechanism for the onset of liquid crystal ordering. Such a view is confirmed by our own experience: We have seen that not only orientational order parameters but also the pitch of twisted nematics induced by chiral solutes can be correctly predicted by the surface tensor model on the basis of the geometrical features of the molecular surface.[8,10,11,23] Now, starting from such a zeroth-order picture, it is worth trying to analyze how the electrostatic interactions can modify the orientational order of solutes. Quantitative information cannot be derived directly from experimental data, since the observed orientational order parameters include contributions from both short-range and electrostatic interactions. Only theoretical models including explicitly the two types of contributions can disentangle their effects on the basis of molecular properties (shape and charge distribution) of the solute. However some suggestion, which needs to be confirmed by using an appropriate model, can be drawn from the comparison of the behavior of the same solute in different solvents. In several cases, it has been observed that at the same reduced temperature, the measured order parameters are shifted in opposite directions on going from a solvent with vanishing dielectric anisotropy to solvents with positive and negative $\Delta\epsilon$ values.[24−28]

In contrast with shape effects for which at least qualitative predictions can be made on the basis of the chemical structure, there is no obvious way to predict how interactions depending on the molecular charge distribution can influence the molecular orientations. Conclusions can be easily drawn only for special cases. A classical example is that of a dipole in a spherical cavity for which, according to the reaction field model, alignment parallel (perpendicular) to the mesophase director is favored in the case of positive (negative) dielectric anisotropy $\Delta\epsilon = \epsilon_{\parallel} - e_{\perp}$.[12,16,17] But real molecules can hardly be represented as spherical objects and the approximation of a dipolar charge distribution is far from general. Therefore the use of a model able to take into account both the molecular shape and the charge distribution in a realistic way is required.

The paper is organized as follows. In section II the theoretical model is described, according to the two contributions, surface tensor and reaction field, to the mean-field potential experienced by a molecule in the nematic phase. The numerical methods employed for the calculation of the mean-field potential are presented in section III by focusing on the electrostatic contributions in nematic phases. The results obtained for some selected solutes, characterized by different charge distributions, in nematic solvents with various dielectric anisotropy are reported and discussed in section IV. Finally, concluding remarks are presented in section V.

II. Mean-Field Potential

The mean-field potential experienced by a molecule in the nematic phase is decomposed as the sum of a short-range contribution, described by the surface tensor model, and an electrostatic term derived according to the reaction field theory. The surface tensor model and the methodology adopted to evaluate electrostatic interactions have been already presented and discussed elsewhere,[8,18] and the reader should refer to the original papers for the details of both. In the following, only the definitions and the most significant features of them will be recalled.

A. Surface Tensor Model. Starting from the consideration that the anisotropy of short-range interactions is determined by the molecular shape and exploiting the analogy with the anchoring free energy of macroscopic surfaces,[29] it is assumed that each (infinitesimal) surface element dS of a molecule tends to orient its normal $\vec{s}$ perpendicular to the director $\vec{n}$ of the mesophase. Such a behavior is accounted for by an energy contribution which, after truncating at the first nonisotropic term the expansion with respect to $\vec{n}\cdot\vec{s}$, is written as $dU_{st} = \xi P_2(\vec{n}\cdot\vec{s})dS$, where P_2 is the second Legendre polynomial and ξ is the temperature-dependent strength of the interaction.[30] The overall potential acting on a molecule is derived by integrating these elementary contributions over the whole molecular surface

$$U_{st}(\omega) = \xi \int_S P_2(\vec{n}\cdot\vec{s})\, dS \tag{1}$$

Its orientational dependence is parameterized according to the polar angles $\omega = (\theta,\varphi)$ of the director with respect to a fixed molecular frame, and it can be specified as

$$U_{st}(\omega) = -\xi \sum_m T^{2,m^*} C_{2m}(\omega) \tag{2}$$

where $C_{Lm}(\omega) = \sqrt{4\pi/(2L+1)}\,Y_{Lm}(\omega)$ are modified spherical harmonics[31], and $T^{2,m}$ are irreducible spherical components of a traceless second rank-tensor denoted as surface tensor

$$T^{2,m} = -\int_S^{C_{2m}}(\theta_s,\varphi_s)\, dS \tag{3}$$

with the polar angles (θ_s,φ_s) identifying the orientation, in the molecular frame, of the normal $\vec{s}$ to the surface element dS. It follows from the definition that the diagonal cartesian component T_{ii} of the surface tensor is related to the anisometry of the molecular surface perpendicular to the i-th molecular axis. A high positive (negative) value of T_{ii} indicates a strong tendency of the molecule to align the i-th axis parallel (perpendicular) to the mesophase director. It follows from the definition that the surface tensor and then the orientational potential $U_{sr}(\omega)$ scales with the overall surface of the molecule. Therefore, a very small short-range contribution to the orienting potential is predicted for small and weakly anisometric molecules.

B. Reaction Field Model. This model describes the electrostatic interactions of a molecule with its environment in terms of the coupling between the molecular charge distribution and the polarization induced in the surrounding dielectric continuum.[12] The system is represented as a charge distribution $\rho(\vec{r})$ in a cavity C bounded by the molecular surface S and surrounded by an infinite dielectric characterized by its permittivity ϵ.[32] In the case of nematics this is an axially symmetric second-rank tensor with its symmetry axis parallel to the director $\vec{n}$. Thus, the electrostatic potential $V(\vec{r})$ has to be derived as the solution of the differential equations

$$-(\partial/\partial\vec{r})\cdot\epsilon\cdot(\partial/\partial\vec{r})V = \rho/\epsilon_0 \text{ outside } C \tag{4a}$$

$$-(\partial/\partial\vec{r})^2\, V = 0 \text{ inside } C \tag{4b}$$

where ϵ_0 is the vacuum dielectric constant. As boundary conditions on the surface S, the continuity on the potential and on the orthogonal component of the electric displacement must be imposed:

$$V_e - V_i = 0 \text{ on } S \tag{5a}$$

$$(\partial V/\partial\vec{r})_i\cdot\vec{s} - (\epsilon\partial V/\partial\vec{r})_e\cdot\vec{s} = 0 \text{ on } S \tag{5b}$$

with the subscripts *e* and *i* denoting the points approaching the surface from outside and inside the cavity, respectively.

The transformation of the differential equations into integral equations on the surface *S* represents a convenient way of solving problems of this kind for cavities of general shape. Standard procedures employing the Green functions for the differential operators of the problem are well known for the case of an isotropic dielectric permittivity, and they allow the evaluation of the polarization energy on the basis of an apparent charge density σ induced on the cavity surface.[12,13] Recently this has been generalized to anisotropic phases by employing the Integral Equation Formalism (IEF).[18,19] In origin, this formalism has been developed for the quantum-mechanical treatment of solvation to evaluate the solvent polarization correction to the solute electronic Hamiltonian in vacuo. We have implemented the same method to describe the interaction between a given charge distribution on the solute molecule and the anisotropic dielectric environment. The theory will not be reviewed here; we shall only recall the main definitions and the final expressions necessary for the following description of its implementation to calculate order parameters.

As mentioned above, the electrostatic problem can be reformulated as the determination of the apparent charge density $\sigma(\vec{r})$ on the surface ($\vec{r} \in S$), through the solution of the equation[18]

$$A\sigma = -g \tag{6}$$

where $g(\vec{r})$ is a function defined on the surface and A an operator on the corresponding functional space, given as

$$A = \left(\frac{1}{2} - D_e\right)S_i + S_e\left(\frac{1}{2} + D_i\right) \tag{7}$$

$$g = \left(\frac{1}{2} - D_e\right)V^0 - S_e E_n^0 \tag{8}$$

In these equations $V^0(\vec{r})$ and $E_n^0(\vec{r})$ are the electrostatic potential and the normal component of the electric field generated by the charge distribution ρ, while S_i, D_i, S_e, D_e are integral operators on the space of functions $u(\vec{r})$ defined on the surface ($\vec{r} \in S$)

$$(S_i u)(\vec{r}) = \int_S G_i(\vec{r},\vec{r}')\, u(\vec{r}')d\vec{r}' \tag{9}$$

$$(D_i u)(\vec{r}) = \int_S u(\vec{r}')\vec{s}(\vec{r})\cdot\left[\epsilon_0 \frac{\partial}{\partial \vec{r}} G_i(\vec{r},\vec{r}')\right]d\vec{r}' \tag{10}$$

$$(S_e u)(\vec{r}) = \int_S G_e(\vec{r},\vec{r}')u(\vec{r}')d\vec{r}' \tag{11}$$

$$(D_e u)(\vec{r}) = \int_S u(\vec{r}')\vec{s}(\vec{r}')\cdot\left[\epsilon_0 \epsilon \frac{\partial}{\partial \vec{r}'} G_e(\vec{r},\vec{r}')\right]d\vec{r}' \tag{12}$$

which employ the Green functions for the electrostatic problem eqs 4a and 4b inside and ouside the cavity

$$G_i(\vec{r},\vec{r}') = \frac{1}{4\pi\epsilon_0|\vec{r} - \vec{r}'|} \tag{13a}$$

$$G_e(\vec{r},\vec{r}') = \frac{1}{4\pi\epsilon_0\sqrt{det(\epsilon)(\vec{r} - \vec{r}')\cdot\epsilon^{-1}\cdot(\vec{r} - \vec{r}')}} \tag{13b}$$

The reaction field contribution to the mean-field potential can then be evaluated as the interaction between the apparent surface charge σ and the molecular charge distribution ρ[12]

$$U_{rf}(\omega) = \frac{1}{2}\int_S V^0(\vec{r})\sigma(\vec{r})dS \tag{14}$$

The angular dependence of U_{rf} in liquid crystal phases derives from the fact that, in view of the anisotropy of the dielectric response of the medium, the apparent surface charge σ depends on the orientation ω of the director. Such an angular dependence is conveniently expressed according to the same modified spherical harmonics of eq 2

$$U_{rf}(\omega) = \sum_{L,m} F^{L,m*} C_{L,m}(\omega) \tag{15}$$

with the coefficients given as

$$F^{L,m} = \frac{2L+1}{4\pi}\int U_{rj}(\omega)\, C_{Lm}^*(\omega)\, d\omega \tag{16}$$

It is worth noticing here that in principle the solution of eq 6 does not present particular problems as long as one can employ standard numerical techniques exploiting the discretization on the boundary surface.[13,14] In practice, however, calculation of the mean-field potential eq 15 is not straightforward for two main reasons. The first reason is that the changes in the reaction field contribution with orientation are rather small if compared with the absolute values of U_{rf}. Therefore, a very accurate calculation of $U_{rf}(\omega)$ is required at each orientation ω to assess its angular dependence. The second reason is that to get a satisfactory sampling of the angular variables in the calculation of the coefficients eq 16, the electrostatic problem has to be repeatedly solved for a large number of ω angles, with overall computation times which may become prohibitively high. The strategy we have adopted to solve the numerical problem will be discussed in section III.

C. Orienting Potential and Order Parameters. The overall orienting potential experienced by a probe molecule in the nematic phase is written as

$$U(\omega) = U_{st}(\omega) + U_{rf}(\omega) = -\xi\sum_m T^{2,m*}\, C_{2m}(\omega) + \sum_{L,m} F^{L,m*}\, C_{Lm}(\omega) \tag{17}$$

In general, the parameter ξ for the strength of the short-range interactions and the dielectric permittivity tensor ϵ, both depending on the temperature, should be evaluated on a molecular basis. Leaving to a future work the study of pure phases, we shall consider here the case of solutes in nematic solvents. If the concentration is low enough, as a first approximation the properties of the solution can be taken to be equal to those of the solvent and parameterized in a simple way. In the present work the Maier−Saupe model has been assumed for the temperature dependence of the orienting strength ξ and the dielectric anisotropy $\Delta\epsilon = \epsilon_{||} - \epsilon_{\perp}$. This means that these properties are assumed to be proportional to the solvent $\bar{P}_2^s$ order parameter, which depends only on the reduced temperature $T^* = T/T^{NI}$, where T^{NI} is the nematic-isotropic transition temperature.[20] For the dielectric permittivity the relation $\Delta\epsilon = \Delta\epsilon^{NI}\bar{P}_2^s/\bar{P}_2^{s,NI}$ is used, with the index *NI* denoting transition values. The form of the orienting strength parameter can be derived from the comparison of the surface tensor potential for solvent molecules, taken as rigid uniaxial objects, $U_s = -\xi T_s^{20} P_2(\cos\theta)$, and the Maier−Saupe expression $U_s = -\xi_0(\bar{P}_2^s T^{NI})P_2(\cos\theta)$, where ξ_0 is a universal constant[20] and T_s^{20} is the only

nonzero component of the surface tensor of the solvent molecules.[8] Thus, the expression $\xi = \xi_0 \bar{P}_2^s T^{NI}/T_s^{20}$ is obtained.

The orientational behavior of molecules in liquid crystal phases is commonly described in terms of order parameters given as the elements of the Saupe ordering matrix $\boldsymbol{S}$:

$$S_{ij} = \frac{1}{2}\int (3n_i n_i - \delta_{ij}) f(\omega)\, d\omega \tag{18}$$

where n_i is the component of the mesophase director along the i-th molecular axis and $f(\omega)$ is the orientational distribution function

$$f(\omega) = \frac{\exp[-U(\omega)/k_B T]}{\int \exp[-U(\omega)/k_B T] d\omega} \tag{19}$$

Since the $\boldsymbol{S}$ matrix is traceless, only two principal values are independent, for instance, S_{yy}, giving the degree of order for the y molecular axis, and the difference $S_{zz}-S_{xx}$, measuring the biaxiality of order perpendicular to this axis.

III. Numerical Procedure

According to eq 17, the molecular properties characterizing the mean-field potential experienced by a given solute are its surface tensor components, $T^{2,m}$, and the expansion coefficients of the electrostatic contribution, $F^{L,m}$. They are calculated on the basis of the molecular surface and of the molecular charge distribution, which we have parameterized as point charges on the atoms. The whole calculation requires the following steps:

A. geometry optimization of the molecule and evaluation of the point charges,

B. definition of the molecular surface,

C. calculation of the surface tensor,

D. matrix representation of the reaction field problem,

E. calculation of the angular dependence of the reaction field potential,

F. calculation of order parameters.

The various steps will be briefly illustrated in the following with more details for items D and E.

A. Geometry Optimization of the Molecule and Evaluation of the Point Charges. Standard quantum mechanical methods are used (i) to optimize the geometrical structure of the solute, required for the definition of its molecular surface, and (ii) to obtain the molecular charge distribution. Geometry optimization is performed at the Hartree−Fock (HF)/6-31G* level following the analytical gradient procedure available in the GAUSSIAN98 package.[33] A point charge representation at the atomic positions is adopted for the molecular charge distribution $\rho(\vec{r})$. This is obtained by applying the Merz−Singh−Kollman scheme[34] to the HF/6-31G* electrostatic potential: the potential is evaluated on a grid of points on the van der Waals surface and a least-squares fitting procedure is used to obtain a set of charges that reproduce as closely as possible the potential at grid points.

B. Definition of the Molecular Surface. The molecular surface defined according to the rolling sphere model is used: This is the surface drawn by a probe of given radius rolling over the envelope of van der Waals spheres centered at the nuclear positions.[35] This definition provides a reasonable representation of the solute surface in contact with the solvent, with smoothed contours and without reentrant parts that are not accessible to solvent molecules of realistic size.

Various rolling sphere algorithms have been proposed; some of us recently implemented one version, based on the Connolly procedure.[23] In all cases, the smoothed molecular surface is made of spherical and toroidal patches, which are then partitioned in a set of triangles (tesserae). The main difference between algorithms is the way of handling the singularities deriving form self-intersecting parts of the surface. The present calculations were performed by using the MSMS code developed by Sanner et al., which is freely available.[36] The input parameters are the nuclear positions, the rolling sphere radius R and the vertex density on the molecular surface.

The same surface has been used for the surface tensor and the electrostatic calculations. Atomic van der Waals radii taken from ref 37 and a rolling sphere radius $R = 3$ Å[23] have been used. A vertex density equal to 5 Å^{-2}, which corresponds to about 2000 tesserae for a molecule such as anthracene, ensures convergence of both the surface tensor and the apparent surface charge. With this choice the coefficients $T^{2,m}$ and $F^{L,m}$ with $L > 0$, corresponding to the anisotropic part of the electrostatic potential see eq 17, are calculated with accuracies of the order of 0.1 Å^2 and some J mol^{-1}, respectively. Note that the number of tesserae is much larger than usually adopted in solvation studies.[19] As a matter of fact, high accuracy is required in our case as a consequence of the weakness of the electrostatic interaction anisotropy.

C. Calculation of the Surface Tensor. As explained in refs 8 and 23, the surface tensor $\boldsymbol{T}$ is calculated as the sum of contributions deriving from each of the tesserae in which the molecular surface is partitioned. The values of the surface tensor components obtained in this work by using the Sanner surface[36] and those calculated with our implementation of the Connolly algorithm[23] show negligible differences provided that in both cases an adequate density of tesserae is chosen.

D. Matrix Representation of Reaction Field Problem. As in the original reference,[19] the surface charge σ is obtained by solving eq 6 with a standard technique in physics and engineering, known as the Boundary Element Method (BEM). This corresponds to a discretization of the problem by partitioning the surface into a finite number N of portions called tesserae, on which a constant charge density is assumed. In this way the integral equation is transformed into an algebraic linear equation of order N. In particular, eq 14 for the reaction field contribution can be rewritten as

$$U_{rf}(\omega) = -\boldsymbol{v}^T \boldsymbol{\sigma} \tag{20}$$

where $\boldsymbol{\sigma}$ is the array collecting the values of the surface charge densities $\sigma_k = \sigma(\vec{r}_k)$ at the centers of the tesserae $\vec{r}_k$, and the transposed array $\boldsymbol{v}^T$ has elements $v_k = -a_k V^0(\vec{r}_k)/2$ where a_k is the surface area of the k-th tessera. An explicit relation for such a contribution

$$U_{rf}(\omega) = \boldsymbol{v}^T \boldsymbol{A}^{-1} \boldsymbol{g} \tag{21}$$

is recovered by discretizing eq 6 as $\boldsymbol{A}\sigma = -\boldsymbol{g}$ in correspondence of the tesserae, with the array $\boldsymbol{g}$ and the square matrix $\boldsymbol{A}$ given as

$$\boldsymbol{g} = (\boldsymbol{1}/2 - \boldsymbol{D}_e)\boldsymbol{V}^0 - \boldsymbol{S}_e \boldsymbol{E}_n^0 \tag{22}$$

$$\boldsymbol{A} = (\boldsymbol{1}/2 - \boldsymbol{D}_e)\boldsymbol{S}_i + \boldsymbol{S}_e(\boldsymbol{1}/2 + \hat{\boldsymbol{D}}_i) \tag{23}$$

In these equations $\boldsymbol{V}^0$ and $\boldsymbol{E}_n^0$ are the arrays having as elements the molecular charge potential $V^0(\vec{r}_k)$ and the corresponding normal component $E_n^0(\vec{r}_k)$ of the electric field at the centers of the surface tesserae. The square matrices $\boldsymbol{S}_i$, $\hat{\boldsymbol{D}}_i$, $\boldsymbol{S}_e$, and $\boldsymbol{D}_e$ derive from the discretization of the integral equations and their

elements are given as

$$S_i^{kk'} = \begin{cases} S_i^{kk'} = a_{k'}/4\pi\epsilon_0|\vec{r}_{kk'}| & k \neq k' \\ \dfrac{1}{4\pi\epsilon_0}\displaystyle\int_{S_k}\frac{1}{|\vec{r}-\vec{r}_k|}dS_k & k = k' \end{cases} \tag{24}$$

$$D_i^{kk'} = \begin{cases} a_{k'}(\vec{r}_{kk'}\cdot\vec{s}_k)/4\pi|\vec{r}_{kk'}|^3 & k \neq k' \\ 0 & k = k' \end{cases} \tag{25}$$

$$S_e^{kk'} = \begin{cases} a_{k'}/4\pi\epsilon_0\sqrt{(\det\epsilon)(\vec{r}_{kk'}\cdot\epsilon^{-1}\cdot\vec{r}_{kk'})} & k \neq k' \\ \dfrac{1}{4\pi\epsilon_0}\displaystyle\int_{S_k}\frac{1}{\sqrt{\det(\epsilon)(\vec{r}-\vec{r}_k)\cdot\epsilon^{-1}\cdot(\vec{r}-\vec{r}_k)}}dS_k & k = k' \end{cases} \tag{26}$$

$$D_e^{kk'} = \begin{cases} a_{k'}(\vec{r}_{k'}\cdot\vec{s}_{k'})/4\pi[\sqrt{(\det\epsilon)(\vec{r}_{kk'}\cdot\epsilon^{-1}\cdot\vec{r}_{kk'})}]^3 & k \neq k' \\ 0 & k = k' \end{cases} \tag{27}$$

where $\vec{r}_{kk'}$ is defined as $\vec{r}_{kk'} = \vec{r}_k - \vec{r}_{k'}$ and $\vec{s}_k$ is the normal outward pointing unit vector of the k-th tessera. The expressions for the off-diagonal elements of the matrices $\boldsymbol{S}_{i(e)}$ and $\boldsymbol{D}_{i(e)}$ are analogous to those reported in ref 19. On the contrary, calculation of the integrals defining the diagonal elements can be greatly simplified in our case by exploiting the fact that tesserae are planar. In particular, the $D_{i(e)}^{kk}$ elements vanish because the relation $(\vec{r}-\vec{r}_k)\cdot\vec{s}_k = 0$ holds over the surface of a tessera, while each of the elements $S_{i(e)}^{kk}$ is conveniently evaluated as the sum of three line integrals, in correspondence with the three triangles with a common vertex at the center in which a tessera can be partitioned.

E. Calculation of the Angular Dependence of the Reaction Field Potential. In principle, the reaction field energy eq 21 can be derived by inversion of matrix $\boldsymbol{A}$, but this would be computationally too expensive from both the points of view of memory requirement (full storage of the matrix or its inverse) and computer time (which scales as N^3). A much more efficient procedure is recovered by employing iterative methods like the Lanczos algorithm[38] or the conjugate gradient,[39] which generate approximations of increasing accuracy by projecting the algebraic problem onto the sequence of Krilov subspaces.[40] Since the real matrix $\boldsymbol{A}$ is not symmetric, one must use the biorthonormal form of these procedures in relation to the two sets of Krilov subspaces generated by the powers of $\boldsymbol{A}$ acting on $\boldsymbol{g}$ as starting vector and the powers of $\boldsymbol{A}^T$ acting on $\boldsymbol{v}$ as starting vector. More specifically, we have implemented the biconjugate gradient algorithm described in ref 41 which, from the initial guesses $\boldsymbol{x}^{(0)}$ and $\tilde{\boldsymbol{x}}^{(0)}$ for the solutions of the two linear systems of equations

$$\begin{aligned} \boldsymbol{A}\boldsymbol{x} &= \boldsymbol{g} \\ \boldsymbol{A}^T\tilde{\boldsymbol{x}} &= \boldsymbol{v} \end{aligned} \tag{28}$$

generates iterative approximations $\boldsymbol{x}^{(i)}$ and $\tilde{\boldsymbol{x}}^{(i)}$ of the i-order, with the corresponding residuals

$$\begin{aligned} \boldsymbol{r}^{(i)} &= \boldsymbol{g} - \boldsymbol{A}\boldsymbol{x}^{(i)} \\ \tilde{\boldsymbol{r}}^{(i)} &= \boldsymbol{v} - \boldsymbol{A}^T\tilde{\boldsymbol{x}}^{(i)} \end{aligned} \tag{29}$$

The convergence of the procedure is conveniently checked by examining the residuals, and we have employed the following criterion for the last iteration:

$$\tilde{\boldsymbol{r}}^{(i)T}\boldsymbol{r}^{(i)}/\boldsymbol{v}^T\boldsymbol{g} \leq 10^{-6} \tag{30}$$

with an estimated relative error on the energy U_{rf} of the same order of magnitude. It should be emphasized that in conjugate gradient methods, and the Lanczos algorithms as well, that rely on the construction of Krilov subspaces, only the vector storage is strictly required since no matrix transformation is performed. Then the full matrix storage can be avoided if its elements can be easily generated when they are needed. This is the case for the off-diagonal elements of matrices $\boldsymbol{S}_\mathbf{i}$, $\hat{\boldsymbol{D}}_\mathbf{i}$, $\boldsymbol{S}_\mathbf{e}$, and $\boldsymbol{D}_\mathbf{e}$, and only their diagonal elements are stored. Correspondingly, any product of $\boldsymbol{A}$ with an array is evaluated according to the right-hand side of eq 23 by performing separately each multiplication of a matrix with a vector.

To characterize the angular dependence of the reaction field contribution $U_{rf}(\omega)$, the electrostatic calculation must be repeated on a grid of orientations ω. The corresponding changes of U_{rf}, and of the solutions $\boldsymbol{x}$ and $\tilde{\boldsymbol{x}}$ of the linear systems eq 28 as well, are rather small. Then one can employ the converged solutions $\boldsymbol{x}$ and $\tilde{\boldsymbol{x}}$ as initial guesses $\boldsymbol{x}^{(0)}$ and $\tilde{\boldsymbol{x}}^{(0)}$ for a nearby orientation. This leads to a significant savings of computation time because of the small number of iterations (usually $M = 1\div3$) necessary to achieve convergence. It should be recalled that the computation time of the conjugate gradient algorithm scales as MN^2, with a saving on the order of M/N with respect to the full inversion of matrix $\boldsymbol{A}$. Of course, no initial guess is available for the first angular calculation (in which case $\boldsymbol{x}^{(0)}$ and $\tilde{\boldsymbol{x}}^{(0)} = \boldsymbol{0}$ is employed) and, correspondingly, a larger number of iterations of the order $M = 10\div20$ is required.

Finally, the coefficients $F^{L,m}$ are derived from eq 16, with the integrals evaluated according to Gauss quadrature formulas[42] by using Legendre and Chebyshev polynomials as weight functions for the variables $x = \cos(\theta)$ and φ, respectively. Calculations were performed by taking 6 points in the range $0\div1$ for the x variable and 24 points in the range $0\div2\pi$ for the φ angle. As a check of the numerical procedure, the reaction field energy of a point dipole in the centre of a spherical cavity in an anisotropic dielectric has been calculated, and agreement with standard results[12] has been found.

F. Calculation of Order Parameters. The orientational order parameters are calculated according to the expressions and the parameterization presented in section II.C. Thus, the input parameters are the temperature, T; the nematic-isotropic transition temperature of the solvent, T^{NI}; T_s^{20}, the only nonvanishing irreducible spherical component of the surface tensor of the solvent, assumed as rigid and uniaxial; the average dielectric permittivity $\bar{\epsilon}$ and the transition value of the dielectric anisotropy $\Delta\epsilon^{NI}$ of the solvent.

IV. Results and Discussion

We will discuss the effects of electrostatic interactions on orientational order by considering some simple representative solutes, different in shape and charge distribution. First we shall consider fluoromethane and acetylene, two small molecules with and without dipole moment, whose axially symmetric order parameters have been measured in various nematic solvents.[22] Second, as an example of a nonpolar biaxial molecule, we will examine the case of anthracene, for which many experimental data are available but which are not yet fully explained.[24,43] Finally, we will investigate the effect of the presence of one or more dipoles and of their location in an aromatic system by considering nitrobenzene, *p*-dinitrobenzene, and anthraquinone,

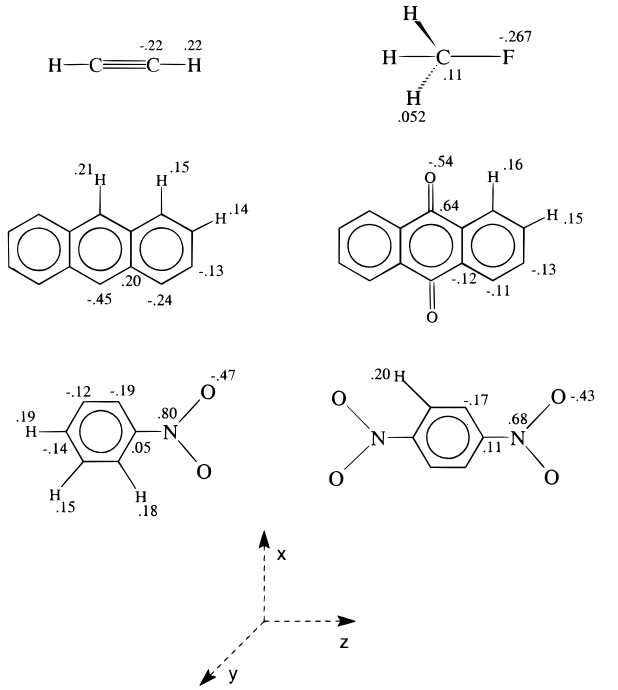

Figure 1. Chemical structure of the solutes considered in the text, with the point charges calculated at the HF/6-31G* level (in atomic unit).

which possess strongly polar groups, although not necessarily the whole molecule is polar.

The chemical structures of the examined solutes are shown in Figure 1, together with the point charges obtained from our calculations and the molecular frame taken as reference. In the case of the molecules with nitro groups, a planar geometry has been considered, and the torsional angle distribution around the C-N bond has been neglected. This is justified by the barrier height of the torsional potential, which is about 12 kJ/mol.[44] It can be seen that typical nonpolar systems also possess nonnegligible charges. Thus, comparable electrostatic effects can be expected in both cases, in contrast with the simplistic assumption that they should be much stronger for polar systems. Table 1 reports the dipole and quadrupole moments calculated from point charges, which are in satisfying agreement with the experimental values.

Electrostatic interaction energies calculated for three different orientations of the molecule with respect to the nematic director, $x//\vec{n}$, $y//\vec{n}$, $z//\vec{n}$, are reported in Table 2. Actually, the differences $\Delta U^i_{rf} = U^i_{rf} - U^i_{rf,0}$ are reported, where U^i_{rf} is the reaction field energy calculated for the orientation with the *i*-th molecular axis parallel to the director in a solvent with average permittivity $\bar{\epsilon}$ and dielectric anisotropy $\Delta\epsilon$, and $U_{rf,0}$ is the interaction energy in a solvent with $\Delta\epsilon = 0$ and the same dielectric constant $\bar{\epsilon}$. Solvents with positive and negative dielectric anisotropies have been considered, with dielectric permittivity values appropriate for 5CB (4-pentyl-4′-cyanobiphenyl, with $\Delta\epsilon = 11.5$) and MBBA (*N*-(4-methoxybenzylidene)-4-*n*-butylaniline, with $\Delta\epsilon = -0.74$), evaluated at a reduced temperature $T/T^{NI} = 0.91$ according to the method outlined in section IIC. The following transition parameters have been assumed: $T^{NI} = 308$ *K*, $\bar{\epsilon}^{NI} = 10.17$, $\Delta\epsilon^{NI} = 8$ for 5CB, and $T^{NI} = 320$ *K*, $\bar{\epsilon}^{NI} = 5.17$, $\Delta\epsilon^{NI} = -0.52$ for MBBA. The magnitude of electrostatic interactions for a given molecule depends upon the value of the average dielectric permittivity, while their orientational dependence is essentially determined by the dielectric anisotropy of the medium. In all cases we have found an almost linear dependence of $U_{rf}(\omega)$ on $\Delta\epsilon$ (for a given value of the average dielectric permittivity $\bar{\epsilon}$), and a negligible contribution of coefficients $F^{L,m}$ with a rank *L* higher then the second. Note that the ΔU^i_{rf} values do not sum to zero. The data on Table 2 point out that the orientational dependence of electrostatic interactions is rather weak, with changes typically smaller than 1 kJ/mol, with effects of opposite sign in solvents having $\Delta\epsilon > 0$ or $\Delta\epsilon < 0$. The fact that the energy differences in Table 2, as well as the changes of order parameters that are described in the following, are much slighter in solvents with negative dielectric anisotropy, is essentially the result of the smaller magnitude of $|\Delta\epsilon|$ in such cases. Of course, the comparison with the anisotropic effects of short range interactions should be performed to assess the effective role of electrostatic interactions in the orientational order. Since typical anisotropies calculated with the surface tensor model range between tenths of kJ/mol to some kJ/mol, depending on the molecular dimensions and the anisometry of the molecular shape, one can anticipate that orientational effects of electrostatic interactions cannot be excluded, even if usually they are smaller in magnitude. A peculiar case is represented by molecules, like acetylene and fluoromethane, whose shape effects are very weak because of their small size. Correspondingly, electrostatic interactions might be predominat by favoring orientations with the symmetry axis parallel to the director for $\Delta\epsilon > 0$ and perpendicular to it for $\Delta\epsilon < 0$ (see Table 2). Therefore, electrostatic interactions alone could explain the experimental observation that the order parameter exhibited by acetylene and fluoromethane is positive in ZLI1132 (a mixture of 4-cyano-(4′-*trans*-*n*-alkylcyclohexyl)benzenes 4-cyano-(4′-*trans*-*n*-pentylcyclohexyl)-biphenyl, with $\Delta\epsilon > 0$) and negative in EBBA (*N*-(4-ethoxybenzylidene)-4-*n*-butylaniline, with $\Delta\epsilon < 0$).[22]

On the contrary the short range interactions play a major role with the other molecules shown in Figure 1, which have an intrinsic biaxiality. By considering only the shape, a similar orientational behavior is expected for the four aromatic molecules, with the long axis preferentially aligned with the director and the normal to the molecular plane perpendicular to the director. This means that shape effects are expected to give the following sequence of principal order parameters: $S_{zz}[>0] > S_{xx} > S_{yy}[<0]$. Such an expectation is confirmed by the analysis of the surface tensor components, reported in Table 3. On the contrary, the effects of elettrostatic interactions are quite different in the four molecules. To characterize them, we shall compare the Saupe ordering matrices calculated for solvents with $\Delta\epsilon = 0$ (in which case only shape interactions are taken into account), $\Delta\epsilon < 0$ and $\Delta\epsilon > 0$. In particular, profiles of the order parameters S_{zz}-S_{xx} vs. S_{yy} will be presented; the latter measures the degree of ordering of the *y* molecular axis perpendicular to the molecular plane, while the former, denoted as the biaxiality order parameter, accounts for the difference in alignment tendency between the principal ordering axes in the molecular plane. In this kind of diagram the temperature is an implicit variable, and the increase of order parameters corresponds to a decrease of temperature. Transition temperature T^{NI} and dielectric permittivity values used in the calculations have been selected by taking again 5CB and MBBA as reference solvents. For the solvent, the value $T^{20}_s = 70$ Å^2, suitable for a typical nematogenic system like 5CB, has been chosen.[45] Order parameters calculated in the range $T/T^{NI} = 0.77 \div 1$ will be considered. Again, opposite changes are predicted in solvents with positive and negative dielectric anisotropy. Therefore in the following discussion only the case $\Delta\epsilon > 0$ will be

TABLE 1: Electric Dipole and Quadrupole Moments Derived from the Point Charges Calculated at the HF/6-31G* Level. Dipole Moments are Given in Debye and Quadrupole Moments in Debye·Å. The Origin of the Molecular Frame is Taken in the Center of Mass of the Molecule[a]

	μ	Q_{xx}	Q_{yy}	Q_{zz}
Acetylene	0.0	−2.49	−2.49	4.98 (3 ÷ 8.4)
Fluoromethane	1.98 (1.85 ÷ 2.05)	−0.13	−0.13	0.26 (−0.4 ÷ 2.3)
Anthracene	0.0	8.61 (10.4)	−17.56 (−18.3)	8.95 (7.94)
Nitrobenzene	5.09 (4.2)	−1.91	6.04	−4.13
p-dinitrobenzene	0.0	20.11	16.19	−36.30
Anthraquinone	0.0	−21.66	−11.15	32.81

[a] Experimental values in parentheses.[12,16]

TABLE 2: Electrostatic Interaction Energy U^i_{rf}, $i \in \{x,y,z\}$, in a Solvent with Average Dielectric Permittivity $\bar{\epsilon}$ and Dielectric Anisotropy $\Delta\epsilon$, for the Molecular Orientation $i//\vec{n}$, the Difference $\Delta U^i_{rf} = U^i_{rf} - U_{rf,0}$ is Calculated with Respect to the Interaction Energy $U_{rf,0}$ in the Absence of Dielectric Anisotropy; Energy is Given in J mol^{-1}

	$\bar{\epsilon} = 10.17\ \Delta\epsilon = 0$	$\bar{\epsilon} = 10.17\ \Delta\epsilon = 11.5$			$\bar{\epsilon} = 5.17\ \Delta\epsilon = 0$	$\bar{\epsilon} = 5.17\ \Delta\epsilon = -0.74$		
	$U_{rf,0}$	ΔU^x_{rf}	ΔU^y_{rf}	ΔU^z_{rf}	$U_{rf,0}$	ΔU^x_{rf}	ΔU^y_{rf}	ΔU^z_{rf}
Acetylene	−11829	301	301	54	−9919	−13	−13	59
Fluoromethane	−13652	259	259	146	−11708	−4	−4	38
Anthracene	−28947	527	25	1480	−23931	33	176	−159
Nitrobenzene	−38995	1024	564	552	−33064	−38	67	75
p-dinitrobenzene	−56677	1551	874	456	−47447	−84	58	167
Anthraquinone	−50063	1253	832	514	−42267	−38	59	112

TABLE 3: Components of the Surface Tensor (in Å^2) Calculated for the Planar Aromatic Molecules under Investigation in the Reference Frame Shown in Figure 1

	T_{xx}	T_{yy}	T_{zz}
Acetylene	−3.4	−3.4	6.8
Fluoromethane	−1.2	−1.2	2.4
Anthracene	12.4	−53.0	40.6
Nitrobenzene	8.7	−30.2	21.4
p-dinitrobenzene	8.9	−43.0	34.1
Anthraquinone	18.4	−60.4	42.0

considered, with the implicit assumption that all the deductions should be reversed for a negative dielectric anisotropy.

In the case of anthracene, it can be seen from Table 2 that electrostatic interactions stabilize the perpendicular arrangement, with a strong tendency of the long molecular axis to orient normal to the director. This corresponds to alignment in the direction of higher dielectric permittivity of the axis characterized by the largest component of the electric quadrupole tensor. Therefore, electrostatic interactions have the effect of reducing the biaxiality or ordering in the plane perpendicular to the long molecular axis, as can be seen in Figure 2a. For the sake of comparison, order parameters measured in solvents with different dielectric anisotropies[24]are displayed in Figure 2b; they refer to the solvents PCH7 (4-cyano-(4′-*trans*-heptylcyclohexyl)-benzene, $\bar{\epsilon} \approx 7$, $\Delta\epsilon^{NI} \approx 8$), HAB (4,4′-di-*n*-heptylazoxybenzene, $\bar{\epsilon} \approx 3.5$, $\Delta\epsilon^{NI} \approx 0.2$), Phase V (a commercial mixture of 4-*R*,4′-*R*′-azoxybenzene derivatives, each with dielectric permittivity comparable with that of MBBA, so a small negative dielectric anisotropy is expected) and ZLI1167 (a commercial mixture of alkyl-cyanocyclohexyls, which should then have a dielectric permittivity not very different from that of PCH7). A similar behavior, which can be summarized as a decrease (increase) of the biaxiality of ordering in the molecular plane for solvents with positive (negative) dielectric anisotropy, is also presented by other aromatic nonpolar molecules, such as *p*-xylene[25] or naphthalene.[26] It appears from Figure 2 that both the sign and the order of magnitude of electrostatic effects are correctly predicted by our method. A closer agreement would require a more detailed model for short-range interactions, by overcoming the picture of the solvent as a continuum, which is implicit to the surface tensor model, to account for the molecular structure of the solvent.[46,47] Another, although smaller, possible correction

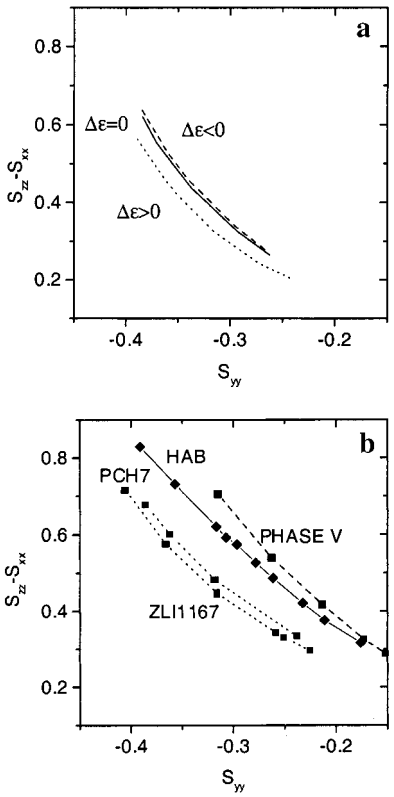

Figure 2. (a) Predicted order parameters for anthracene in solvents with different dielectric anisotropy. (b) Order parameters measured in the nematic solvents ZLI1167, PCH, HAB and Phase V.[24]

should derive from the inclusion in the electrostatic model of the polarizability contribution, which is expected to increase both the reaction field energy and its anisotropy.[12]

When a strong dipole is introduced, as in nitrobenzene, there is a competition between the tendency to the perpendicular alignment of the molecular plane, as observed in anthracene, and that of the dipole to align in the direction of higher dielectric permittivity. The result is that for this molecule the electrostatic interaction energy is practically independent of the director orientation in the *yz* plane, while a net preference for the perpendicular alignment of the *x* axis is predicted. Thus, in

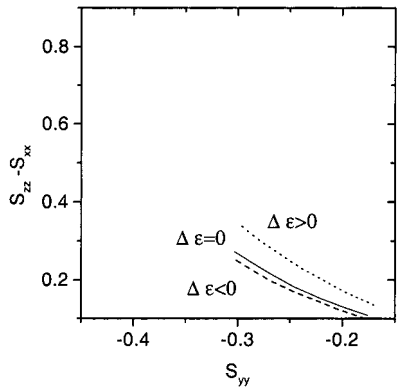

Figure 3. Predicted order parameters for nitrobenzene in solvents with different dielectric anisotropy.

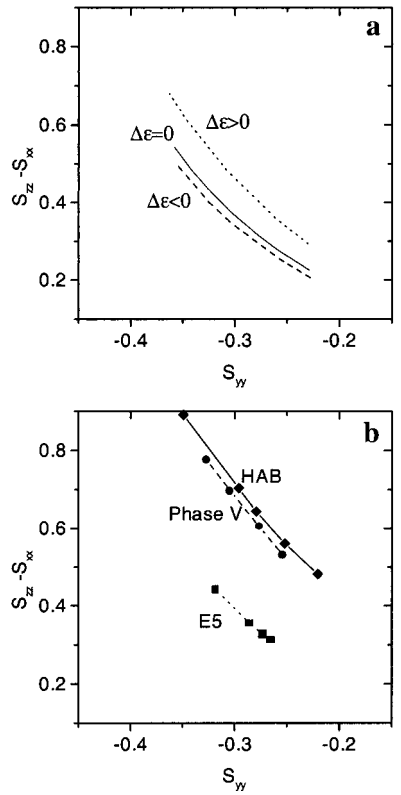

Figure 4. (a) Predicted order parameters for *p*-dinitrobenzene in solvents with different dielectric anisotropy. (b) Order parameters measured in the nematic solvents E5, HAB, and Phase V.[48]

contrast with what seen for anthracene, the biaxiality of ordering in the molecular plane increases in nematic solvents with positive dielectric anisotropy, as shown in Figure 3. The overall decrease of order parameters and the simultaneous strengthening of electrostatic effects, in comparison with anthracene in the same solvents at the same temperatures, is due to the smaller dimension of nitrobenzene, which experiences a weaker short-range orienting potential, as can be seen from the surface tensor values in Table 3.

The presence of the two antiparallel dipoles in the case of *p*-dinitrobenzene favors even more the tendency to align the long molecular axis with respect to the director. Table 2 shows that electrostatic interactions have the effect of stabilizing orientations with the long axis parallel to the director and the *x* axis perpendicular to it, with a corresponding increase of the order biaxiality in the molecular plane, as shown in Figure 4a. Measured order parameters available in the literature[48] are displayed in Figure 4b. It can be seen that, in agreement with the theoretical predictions, the order parameter biaxiality decreases on going from HAB, which has a negligible dielectric anisotropy, to Phase V, which is characterized by a negative dielectric anisotropy. A further and much larger decrease of biaxiality is observed in E5, which is a commercial mixture of alkyl- and alkyloxy-cyanobiphenyls. If, as can be inferred from the composition, this solvent has a positive dielectric anisotropy, the experimental data are at variance with our predictions. Actually, while HAB and Phase V are structurally similar and the differences in solute ordering can be reasonably ascribed to electrostatic interactions, the comparison with E5 is less straightforward. The peculiar behavior of this solvent is confirmed by the fact that even in the case of anthracene the order parameters measured in E9, a mixture with composition similar to E5, do not show the trend generally observed in nematics with positive dielectric anisotropy.[24] Furthermore, in the case of *p*-dinitrobenzene, solvent effects on the torsional potential, modifiying the amplitude of the torsional distribution around the planar minima, and then the effective biaxiality of the molecular shape, cannot be excluded. The available data do not provide a certain answer, and other experiments would be required for a better understanding. Thus, limiting our considerations to the solvents HAB and Phase V, from a comparison between anthracene and *p*-dinitrobenzene we can see that electrostatic interactions have opposite effects on orientational ordering for the two solutes, in agreement with experiment. Also for *p*-dinitrobenzene the biaxiality of ordering appears to be underestimated by our model, and this, as already mentioned, is probably the result of the neglect of short-range correlations between solute and solvent in the surface tensor model.

As a final example, the case of anthraquinone will be considered. It appears from Table 2 that, despite the presence of strong antiparallel dipoles, electrostatic interactions destabilize orientations with the *x* axis parallel to the director, while alignment of the *z* axis is strongly favored. This behavior warns against simple predictions based on the superposition of the expected effects of local dipoles (along the C-O bond in this case). Actually, as for the other nonpolar molecules seen so far, the general trends can be interpreted in terms of the molecular electric quadrupole. Reaction field interactions stabilize the orientations with the major component in the direction of higher dielectric permittivity. The increase (decrease) predicted for the biaxiality order parameters of anthraquinone, when dissolved in nematics with positive (negative) dielectric anisotropy, is shown in Figure 5a. Even in this case the theoretical predictions agree with the experimental results, as appears from Figure 5b which reports order parameters obtained from NMR measures in the nematic solvents ZLI1167[43] and PAA (4,4′-dimethoxyazoxybenzene, $\bar{\epsilon} \approx 5.7$, $\Delta\epsilon^{NI} \approx -0.1$).[49] A comparison with anthracene shows that in the case of anthraquinone the effects are larger and of opposite sign. In particular, the model provides an explanation for the experimental finding that, in contrast with what is expected on the basis of the molecular shape and predicted by the surface tensor model, in a solvent like ZLI1167 anthracene has a more disclike behavior (lower biaxiality of order) than anthraquinone.

V. Concluding Remarks

The mean-field potential proposed here, which is a superposition of a surface tensor and a reaction field contribution, accounting respectively for short-range and electrostatic interactions, predicts small, but nonnegligible effects of electrostatic interactions on the orientational order of solutes in nematics.

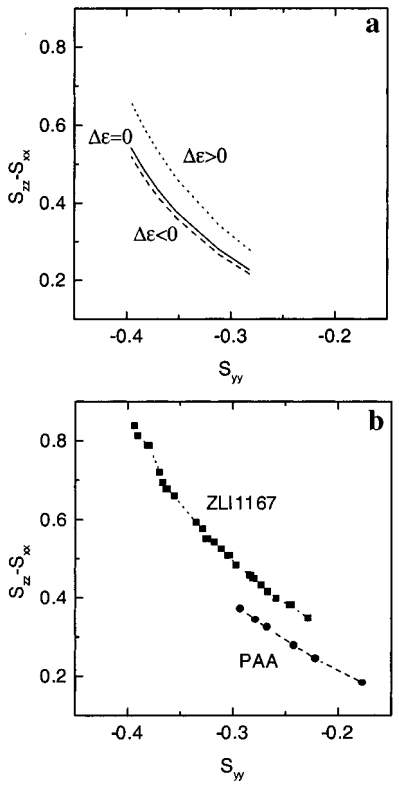

Figure 5. (a) Predicted order parameters for anthraquinone in solvents with different dielectric anisotropy. (b) Order parameters measured in the nematic solvents ZLI1167[43] and PAA.[49]

In particular it has been shown that the model, in which the solvent is characterized only by its dielectric anisotropy, is able to explain solvent effects on solute order parameters. A limit of the present approach can be devised in the inherent approximation of the surface tensor model, which takes into account in a detailed way the structure of the solute, while the coupling with the solvent is simply parameterized according to the Maier-Saupe theory. More accurate predictions could be obtained only by considering the short-range orientational correlation between probe and solvent molecules. This can be done with a van der Waals approach taking into account in an explicit way attractive and repulsive intermolecular interactions and their dependence on the molecular structure.[46,47]

The reaction field technique we have used for the electrostatic interactions, based on a realistic description of the charge distribution and the molecular surface defining the boundary of the cavity that encloses the charges, has been widely used and shown its reliability in the quantum mechanical context of solvation studies.[13] Electrostatic energies in the isotropic phase obtained with our procedure, which assumes a smoothed surface defined according to the rolling sphere algorithm and a point charge distribution, are consistent with those calculated with a standard package for quantum mechanical calculations.[33] It should be emphasized that the method, which does not require the introduction of any free parameter, relies on a detailed description of molecular charge distribution and of molecular surface, whose shape determines how much charges are exposed to solvent. The important role of the shape is illustrated by Table 4, which reports electrostatic interaction energies calculated for the four aromatic molecules by assuming spherical cavities of diameter large enough to contain the van der Waals envelope. From comparison with the data of Table 2, it can be seen that not only energies and energy differences are underestimated, but also their angular dependence can be completely different

TABLE 4: Electrostatic Interaction Energy U^i_{rf}, $i \in \{x,y,z\}$, in a Solvent with Average Dielectric Permittivity $\bar{\epsilon}$ and Dielectric Anisotropy $\Delta\epsilon$, for the Molecular Orientation $i // \vec{n}$ and a Spherical Cavity of Radius R (the Difference $\Delta U^i_{rf} = U^i_{rf} - U_{rf,0}$ is Calculated with Respect to the Interaction Energy $U_{rf,0}$ in the Absence of Dielectric Anisotropy; Energy is Given in J mol^{-1})

		$\bar{\epsilon} = 10.17\ \Delta\epsilon = 0$	$\bar{\epsilon} = 10.17\ \Delta\epsilon = 11.5$		
	R/Å	$U_{rf,0}$	ΔU^x_{rf}	ΔU^y_{rf}	ΔU^z_{rf}
Anthracene	5.75	−3867	113	50	33
Nitrobenzene	4.3	−15504	401	343	105
p-dinitrobenzene	4.88	−20323	614	548	33
Anthraquinone	5.6	−11156	372	288	25

from that predicted when the molecular shape is taken into account. The general effect is a significant reduction of electrostatic energies, which becomes dramatic when the largest charges lie far from the surface of the sphere. Analogously, the importance of a realistic charge distribution has to be stressed. We have seen that the effects cannot be simply explained by dipole interactions. In contrast with the assumption of some authors,[22] we can not even state that quadrupole interactions alone are sufficient to account for all electrostatic effects. Similar conclusions about the importance of shape, of the presence of dipoles and quadrupoles and of their location in the molecule, have been reached by other authors analyzing with a different mean-field approach the effects of electrostatic interactions on ordering of rigid solutes in nematics.[50]

Since the results obtained for orientational ordering of solutes are promising, application of the model presented here to the analysis of other properties of liquid crystals is in order. Encouraging results have been obtained from preliminary calculations of electrostatic effects on the helical twisting power of chiral dopants with similar shapes but different charge distributions. For the near future, application to the prediction of the dielectric permittivity of nematics is planned.

Acknowledgment. The authors gratefully acknowledge financial support from MURST PRIN ex 40%, EC (TMR contract FMRX CT97 0121) and CNR, through its Centro Studi sugli Stati Molecolari.

References and Notes

(1) Onsager, L. *Ann. N. Y. Acad. Sci.* **1949**, *51*, 627.
(2) Maier, W.; Saupe, A. *Z. Naturforsch.* **1960**, *15a*, 287.
(3) Born, M. *Ann. Phys.* **1918**, *55*, 221.
(4) Cladis, P. E. *Mol. Cryst. Liq. Cryst. Technol.* **1988**, *165*, 85.
(5) Goodby, G. W. In *Ferroelectric Liquid Crystals*; Gordon & Breach: Amsterdam, 1991.
(6) McGrother, S.; Gil-Villegas, A.; Jackson, G. *Mol. Phys.* **1998**, *95*, 657.
(7) Dunmur, D. A.; Palffy-Muhoray, P. *Mol. Phys.* **1992**, *76*, 1015. Perera, A.; Patey, G. N. *Phys. Rev. Lett.* **1998**, *60*, 2303. Berardi, R.; Orlandi, S.; Zannoni, C. *Chem. Phys. Lett.* **1996**, *261*, 357.
(8) Ferrarini, A.; Moro, G. J.; Nordio, P. L.; Luckhurst, G. R. *Mol. Phys.* **1992**, *77*, 1.
(9) Ferrarini, A.; Luckhurst, G. R.; Nordio, P. L.; Roskilly, S. J. *J. Chem. Phys.* **1994**, *100*, 1460.
(10) Ferrarini, A.; Moro, G. J.; Nordio, P. L. *Phys. Rev. E* **1996**, *53*, 681; Ferrarini, A.; Moro, G. J.; Nordio, P. L. *Mol. Phys.* **1996**, *87*, 485.
(11) Ferrarini, A.; Nordio, P. L.; Shibaev, P. V.; Shibaev, V. P. *Liq. Cryst.* **1998**, *24*, 219; Ferrarini, A.; Dal Mas, N.; Nordio, P. L.; Styring, P.; Todd, S. M. *Mol. Cryst. Liq. Cryst. Sci. Technol.* **1999**, *328*, 391.
(12) Böttcher, C. J. F.; Bordewijk, P. *Theory of Electric Polarization*; Elsevier: Amsterdam, 1973.
(13) Tomasi, J.; Persico, M. *Chem. Rev.* **1994**, *94*, 2027.
(14) Davis, M.; Mccammon, J. A. *Chem. Rev.* **1990,** *90*, 509.
(15) Rega, N.; Cossi, M.; Barone, V.; Pomelli, C. S.; Tomasi, J. *Int. J. Quantum. Chem.* ***1999***, *73*, 219.
(16) Segre, U. *Mol. Cryst. Liq. Cryst. Sci. Technol.* **1983**, *90*, 239.
(17) Celebre, G.; de Luca, G.; Ferrarini, A. *Mol. Phys.* **1997**, *92*, 1039.

(18) Cancès, E.; Mennucci, B. *J. Math. Chem.* **1998**, *23*, 309.
(19) Mennucci, B.; Cancès, E.; Tomasi, J. *J. Phys. Chem. B* **1997**, *101*, 1056.
(20) Vertogen, G.; de Jeu, W. H. *The Physics of Liquid Crystals, Fundamentals;* Springer: Berlin, 1988.
(21) Emsley, J. W., Ed. *NMR of Liquid Crystals*; Reidel: Dordrecht, The Netherlands, 1985.
(22) Burnell, E.E.; de Lange, C.A. *Chem. Rev.* **1998**, *98*, 2539.
(23) Ferrarini, A.; Janssen, F.; Moro, G. J.; Nordio, P.L. *Liq. Cryst.* **1999**, *26*, 201.
(24) Emsley, J. W.; Hashim, R.; Luckhurst, G. R.; Shilstone, G. N. *Liq. Cryst.* **1986**, *5*, 437.
(25) Emsley, J. W.; Luckhurst, G. R.; Sachdev, H. S. *Mol. Phys.* **1989**, *67*, 160.
(26) Yim, C. T.; Gilson, D. F. R. *J. Phys. Chem.* **1991**, *95*, 980.
(27) Syvitski, R. T.; Burnell, E. E. *Chem. Phys. Lett.* **1997**, *281*, 199.
(28) Cognard, G.; Hieu Phan, T.; Basturk, N. *Mol. Cryst. Liq. Cryst. Sci. Technol.* **1983**, *91*, 327.
(29) Rapini, A.; Papoular, M. *J. Phys. (Paris) Colloq.* **1969,** *30 C 4*, 54.
(30) The parameter ξ is related to the parameter ϵ used in previous works[8] by the relation $\xi = k_B T\epsilon$.
(31) Zare, N. R. *Angular Momentum*; Wiley & Sons: New York, 1987.
(32) Here and in the following we shall indicate as ϵ the relative dielectric permittivity.
(33) Frisch, M. J.; Trucks, G. W.; Schlegel, H. B.; Scuseria, G. E.; Stratmann, R. E.; Burant, J. C.; Dapprich, S.; Millam, J. M.; Daniels, A. D.; Kudin, K. N., Strain, M. C.; Farkas, O.; Tomasi, J; Barone, V.; Cossi, M.; Cammi, R.; Mennucci, B.; Pomelli, C.; Adamo, C.; Clifford, S; Ochterschi, J.; Cui, Q.; Gill, P. M. W.; Johnson, B. G.; Robb, M. A.; Cheeseman, J. R.; Keith, T.; Petersson, Morokuma, K.; Malick, D. K.; Rabuck, A. D.; G. A.; Montgomery, J. A.; Raghavachari, K.; Al-Laham, M. A.; Zakrewski, V. G.; Ortiz, J. V.; Foresman, J. B.; Cioslowski, J.; Stefanov, B. B.; Nanayakkara, A.; Liu, J.; Liashenklo, A; Piskorz, P.; Komaromi, I.; Challacombe, M.; Peng, C. Y.; Ayala, P. Y.; Chen, W.; Wong, M. W.; Andres, J. L.; Replogle, E. S.; Gomperts, R.; Martin, R. L.; Fox, D. J.; Binkley, J. S.; DeFrees, D. J.; Baker, J.; Stewart, J. P.; Head-Gordon, M.; Gonzalez, C.; Pople, J. A. *GAUSSIAN98 (Revision A.6)*, Gaussian, Inc.: Pittsburgh, PA, 1998.
(34) Besler, B. H.; Merz, K. M.; Kollman, P. A. *J. Comput. Chem.* **1990**, *11*, 431. Sigh, U. C.; Kollman, P. A. *J. Comput. Chem.* **1984**, *5*, 129.
(35) Richards, F. M. *Ann. Rev. Biophys. Bioeng.* **1977**, *151*, 6; Connolly, M. L. *J. Appl. Crystallogr.* **1983**, *16*, 548.
(36) Sanner, M. F.; Spenher, J.-C.; Olson, A. J. *Biopolymers* **1996**, *38*, 305.
(37) Bondi, A. *J. Phys. Chem.* **1964,** *68*, 441.
(38) Parlett, B. N. *The Symmetric Eigenvalues Problem*; Prentice Hall: Englewood Cliffs, NJ, 1980; Cullum, J.; Willoughby, R. *Lanczos Algorithm for Large Symmetric Eigenvalue Computations, Theory;* Birkhauser: Basel Switzerland, 1985.
(39) Golub, G. H.; van Loan, C. F. *Matrix Computations*; John Hopkins University Press: Baltimore, 1983.
(40) Vorobyev, Yu. V. *Methods of Moment in Applied Mathematics*; Gordon & Breach: New York, 1965.
(41) Barrett, R.; Berry; M., Chan, T. F.; Demmel; J., Donato, J. M.; Dongarra, J.; Eijkhout, V.; Pozo, R.; Romine, C.; Van der Vorst, H. *Templates for the Solution of Linear Systems: Building Blocks for Iterative Methods*; SIAM: Philadelphia, 1994.
(42) Press, W. H.; Flannery, B. P.; Teukolsky, S. A.; Vetterling, W. T. *Numerical Recipes*; Cambridge University, Cambridge U.K., 1988.
(43) Tarroni, R.; Zannoni, C. *J. Phys. Chem.* **1996**, *100* , 17157.
(44) Janssen, R. H. C.; Theodorou, D. N.; Raptis, S.; Papadopoulos, M. G. *J. Chem. Phys.* **1999**, *111*, 9711.
(45) Ferrarini, A.; Moro, G. J.; Nordio, P. L. In *Physical Properties of Liquid Crystals*, Dunmur, D., Fukuda, A., Luckhurst, G. R., Eds. EMIS Datareviews Series, IEE: London, in press.
(46) Gelbart, W. M. *J. Phys. Chem.* **1982**, *86*, 4298.
(47) Ferrarini, A.; Moro, G. J. In preparation, 2000.
(48) Emsley, J. W.; Hashim, R.; Luckhurst, G. R.; Rumbles, G. N.; Viloria, F. N. *Mol. Phys.* **1983**, *49*, 1321.
(49) Emsley, J. W.; Heeks, S. H.; Horne, T. J.; Howells, M. H.; Moon, A.; Palke, W. E.; Patel, S. U.; Shilstone, G. N.; Smith, A. *Liq. Cryst.* **1991**, *9*, 649.
(50) Terzis, A. F.; Photinos, D. J. *Mol. Phys.* **1994**, *83*, 847.
(51) Gray, G. G.; Gubbins, K. E. *Theory of Molecular Fluids*; Clarendon: Oxford, U.K., 1984.